Chapter

Microstructural and High Temperature Wear Characteristics of Plasma Transferred Arc Hardfaced Ni–Cr–Si–B-C Alloy Deposits

S. Gnanasekaran, Samson Jerold Samuel Chelladurai, G. Padmanaban and S. Sivananthan

Abstract

Due to the tough working environments, wear damage to nuclear reactor components is frequent. Usually, nuclear elements run at 573 k to 873 k. The feed water controller valves, used for the thundering of coolant flow, wear out faster among the reactor components. Austenitic stainless steels, using different methods for hardfacing, improve wear resistance to the cobalt and nickel alloys. Nickel based hardfacing is more resistant to wear than cobalt based hardfacing at high temperatures thanks to the solid oxide layers. Austenitic stainless-steel substrates generally favor nickel-based hardfaced (Ni–Cr-Si–B-C) over cobalt-driven hardfacing because this reduces radiation-induced nuclear activity. A well-known surface method for depositing nickel hardfacing, minimal dilution, alloys is the Plasma Transfer Arc (PTAs) weld technique. In this study the Ni-based alloy is hardfaced over a 316 L (N) ASS substratum with PTA hardfacing, for a dense of approximately 4–4.5 mm. The substrates and deposits were tested at different temperatures with a pin on disc wear (room temperature, 150 and 250°C).When grinding with 1000 grain SiC abrasive paper, the wear test samples were polished to the roughness value (Ra) of less than 0,25 m.The deposit showed a variety of wear mechanisms regarding the test temperature. Using friction and wear values and wear analysis, the wear mechanisms were determined. There was a considerable wear loss at room temperature (RT).At 423 K operating heat, mild ploughing at short sliding distances and tribo-oxidation were carried out with increasing sliding time.The primary wear mechanism was adherence at the time of operating temperature at 623 K, but as the sliding distance widened, tribo-oxidation improved. In combination with a working hardened substrate, the formation of an oxide layer could significantly reduce the wear loss of nickel-based alloys.

Keywords: Austenitic stainless steel, PTA hardfacing, Wear, Microstructure

1. Introduction

Austenitic type 316 L (N) is commonly used in fast-breeder (FBR) reactors at temperatures between 573 K and 874 K as structural material. Austenitic stainless

steels are very resistant to wear under dry sliding conditions [1]. Nickel and cobalt alloys are recommended to be used as layer materials for deposition on austenitic stainless steels using different layering methods to increase wear resistance [2–5]. The soldering technique Plasma Transferred Arc (PTA) is known for depositing nickel and cobalt hard façade alloys with limited dilution on rust-resistant stainless-steel substrates. Nickel-based hard coating on austenitic stainless-steel substrates is commonly a suitable alternative to cobalt-based coating for use in the nuclear industry to minimize radiation-inducing activity [6–8].

Many laboratory experiments have been performed on nickel-based hardfacing alloys as these alloys are both corrosion and oxidation resistant. Kashani et coll. [9] contrasted the use efficiency of room temperature(RT) and high temperature (HT) nickel and cobalt-based hard-facing coatings (823 K). Due to the lightweight oxide layers, they were found to be more wear-resistant to nickel coatings than to cobalt coatings at high temperatures [10]. The wearing conduct of RT, 373, 473, 498, 523 and 623 K of a Deloro 50 hardfacing alloy was investigated. They found the serious Space temperature wear loss (RT). However, the wear loss decreased to near zero at 623 K as the test temperature rose. They suggested to use a nickel-based hardfacing alloy for applications in nuclear power plants where the working temperature is high enough to produce oxidative wear. Berns et al. [11, 12] Hardness test during slipping at high test temperatures witnessed coating operation. In combination with a working hardened substrate, the forming of an oxide layer could greatly minimize the wear loss of nickel-based alloys. Coating sliding can show a variety of wear appliances at different trial temperatures and ranges [13]. Consequently, room and high temperature wear behaviors, using the high-temperature pin-on-disk wear test process, of a Colmonoy 5 hardfacing alloy dropped on a 316 L (N) stainless steel substratum were examined.

2. Experimental work

2.1 Substrate (Base metal) and hardfaced powder (colmonoy-5) properties

AISI 316 LN is an austenitic nuclear-grade stainless steel widely used in valves, valve cones, spins and other structural grain stalks. A vacuum spectrometer determined the chemical composition of the base metal. Sparks of the base metal were ignited at various locations. The resulting spectrum has been studied to estimate alloying components. **Tables 1** and **2** illustrate the chemical compositions of base metal and powder. The content of the foundation was rolling 12 mm thick. The experiments were carried out using a semi-automated PTA tool. The tests were performed by creating a negative electrode charged layer (DCEN). As blinding gas and as powder feed gas, pure argon (99.9 percent) gas was used.

Table 3 displays the configured parameters of the PTA hardfacing mechanism for this study. The deposits were faced with four degrees of principal arc current, while all other parameters were kept stable. The hardfaced samples are seen in **Figure 1**. The deposit was reduced for the study of metallography into small samples after hard-facing. The hardness of the cross section of the repository was tested with a 0.05 sec, with a dwell time of 15 s and a Vickers microhardness measuring press, (Make: SHIMADZU, Japan; Model: HMV2T).

C	Ni	Cr	Mo	Si	Mn	Cu	Nb	S	P	W	Fe
0.020	12.55	17.27	2.35	0.29	1.69	0.047	0.02	0.027	0.026	0.03	**Bal**

Table 1.
Chemical composition wt% of 316LN (Substrate).

C	Fe	Cr	Si	B	O	Ni
0.41	3.10	10.44	4.02	2.26	0.03	**Bal**

Table 2.
Chemical composition of colmonoy-5 (Hardfaced powder).

S.No	Main parameters	Values
1	Main arc current (Amps)	130
2	Traverse speed (mm/min)	160
3	Powder feed rate (grams/min)	35
4	Torch oscillation width (mm)	10
5	Preheating temperature (°C)	400

Table 3.
PTA process parameters used for hardfacing.

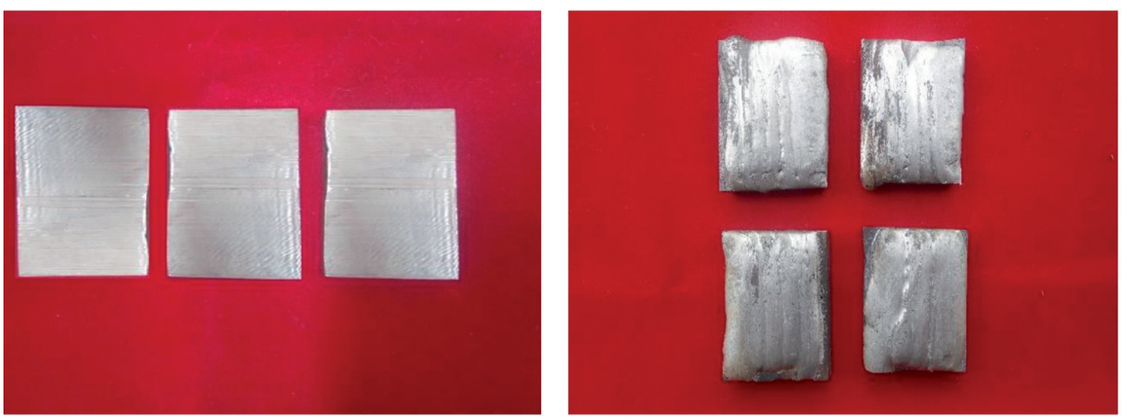

Figure 1.
Photograph of hardfaced specimens. (a) Before hardfacing. (b) After hardfacing.

Parameters	Values
Pin	D = 10 mm, L = 20 mm
Disc	D = 160 mm, W = 8 mm
Load	50 N
Velocity Range	1 m/s
Sliding distance	450 m, 800 m, 1200 m, 1600 m

Table 4.
Wear test parameters.

The specimens were separated to the required size and polished with different grades of emery paper for metallographic inspection. A typical reagent of 0.25 g, 20 ml ethanol and 1.25 ml of HCL were used to detect the microstructure of the specimens. The microstructural research has been carried out using the optical light-emitting microscope (OM) (Make: MEIJI, Japan; Model: MIL7100) (Metal Vision). Pin-on disc wear experiments were carried out at three different temperatures for the layer and deposit (room temperature, 423 K, and 623 K) (**Table 4**).

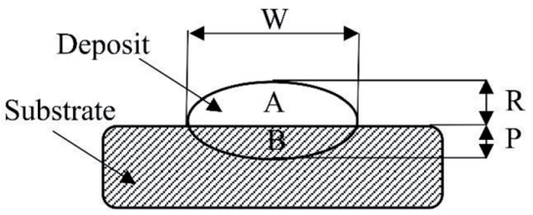

Where,

P - Penetration
R - Reinforcement
W - Width
A - Reinforcement area
B - Penetration Area

Figure 2.
Bead profile and bead geometries.

2.2 Dilution

The welding method with the least dilution is generally favored for tough applications. Dilution is the proportion of the base metal in a metal deposit. As the dilution increases, the amount of base metal in the welded metal deposit increases and vice versa. Hardfacing is achieved mainly to enhance the base metal (substrate) surface properties. Hardfaced surfaces usually outperform the wear, degradation and oxidation resistance of base metals. The surface properties do not change to the expected degree in higher dilution rates because of the inclusion of a larger volume of base metal. This section performed an experimental study to assess the dilution percentage at different power levels. After hardfacing, the specimens were selected from the centre of the deposit. Metallographic technique and specimens of 2% Nital were used to polish the surface of the material. In high-resolution scanners the bead profile and geometry as seen in **Figure 2** was visualized and registered. Dilution was calculated using the following expression.

$$\text{Dilution}\,(\%) = \frac{B}{A+B}\ \text{x}\ 100\% \qquad (1)$$

3. Results and discussion

3.1 Characterization of the deposits

At higher transferred arc currents, heat generation is higher and the material is melted after the powder excess heat. In addition, increased arc forces improve heat generation, which increases the penetration depth of the substrate material. The heat generation is lowers at lower transferred arc currents and the rest of the heat generation is used to melt the powder, allowing less heat to melt the base material after melting the powder. In addition, the arc force in this state is decreased and the penetration depth and superficial penetration decrease. Dendritic nickel growth nearly perpendicular to the deposit interface with a greater magnification has been detected (**Figure 3a**). The microstructure of the deposits includes -nickel dendrites with precipitation of interdendritic carbide. The deposit near the interface is significantly different from the top of the cover (**Figure 3b**).

Figure 4 displays the hard-faced deposit scanning electron micrograph consisting of the nickel solid solution phase dendrites and the eutetic mixture as interdendritic components. The average hardness of the deposit is approximately 530 HV, and is held at 1 mm from the interface. Basic metals have an average hardness of around 250 HV. The Colmonoy 5 coatings have averaged two times higher hardness relative to the substrate. The existence of an evenly dispersed blend of complex carbohydrates and borides causes the improved stiffness of the overlays (**Figure 5**).

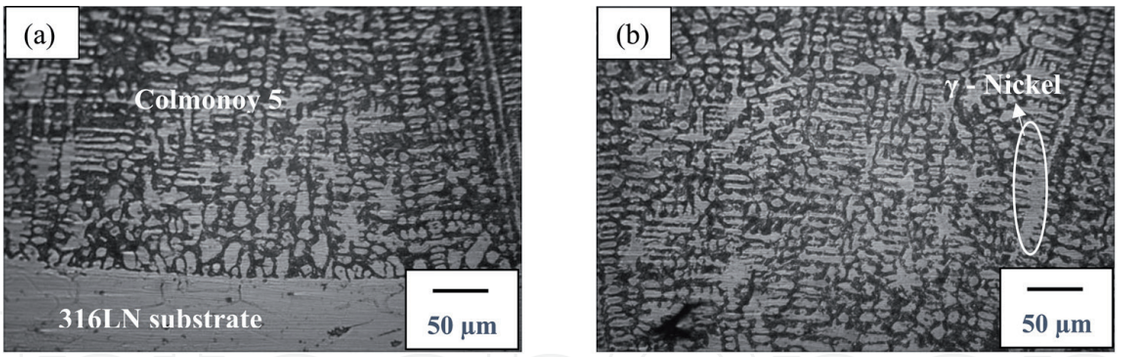

Figure 3.
Optical micrographs of (a) Interface with etching and (b) hardfaced deposit.

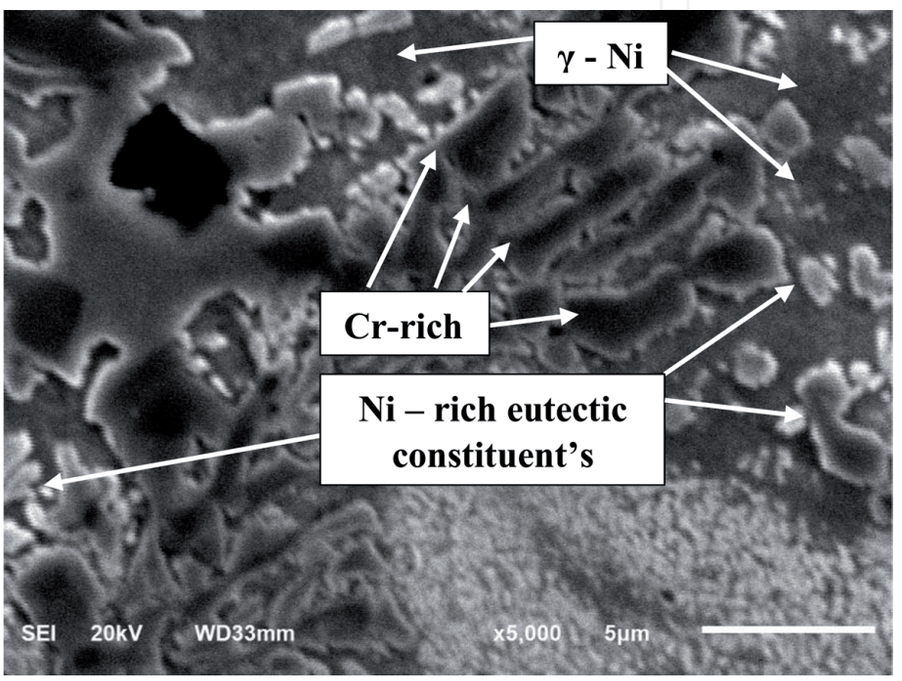

Figure 4.
Scanning electron micrograph - Cr-rich precipitates.

3.2 Dry sliding wear behavior

The apparel of the depot is seen in **Figure 6** due to test temperatures in different sliding lengths. Wear loss is evident as sliding distance increases and the test temperature decreases. RT inspections indicate further wear loss on the deposit. Wear loss decreased at 423 K and 60–75% at 623 K at higher test temperatures by 20–30 percent in comparison with RT samples. The estimated deposit wear ratios at RT, 423 K and 623 K are 3.01, 2.1 and 1.07 g/Nm. Due to the development of smoothly crushed oxide layers on sliding sides, apparel loss of the nickel-based hardfaced alloy may be reduced as stated in detail [14]. In the incidence of the oxygen atmosphere, oxide layers are more readily formed in contact areas that have been locally adjusted due to the superimposed operating temperature and frictional temperature effects. The highest wear loss (60–70%) for 1600 m of sliding reserve was found throughout the running age during RT experiments. The plan of harsh stringencies and the combination of apparel debris, which led to scratch and investing of all sliding sides, caused the severe wear during the run-in period [15].

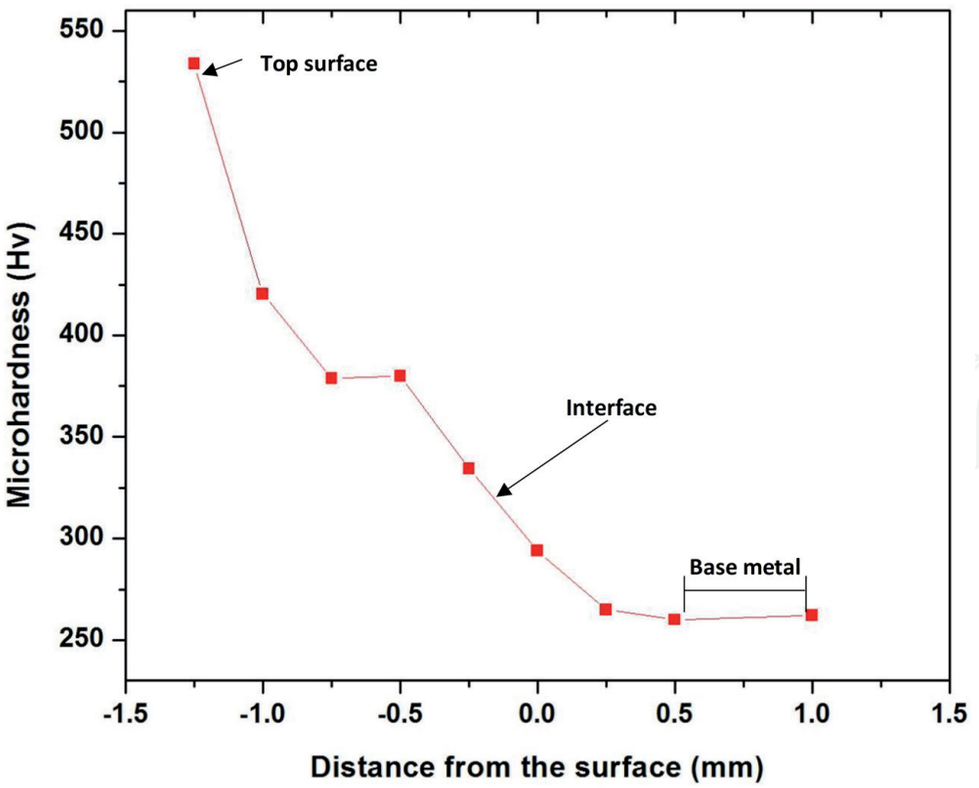

Figure 5.
Stability distribution between substrate and deposit.

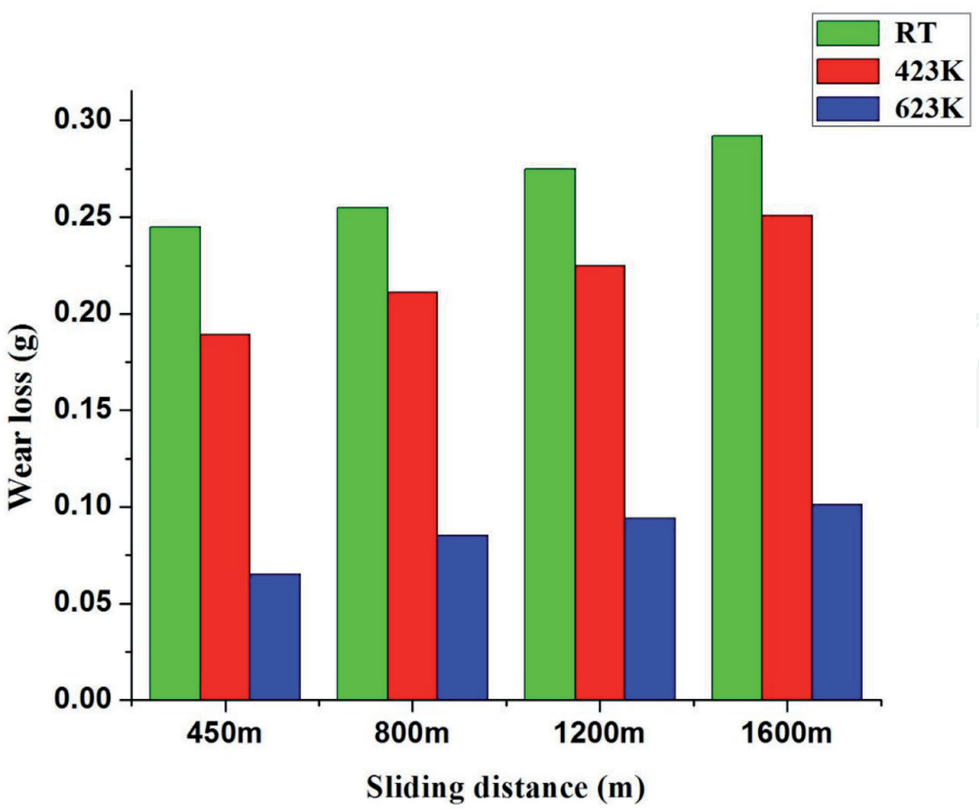

Figure 6.
Outcome of test temperature on wear loss of the deposit at unlike sliding distances.

3.3 Dry sliding friction behavior

The sliding distance is compared to the operational and stable friction coefficient (COF) morals during RT and at extraordinary temperatures in **Figure 7**. The COF development with a sliding distance is highly temperature dependent. At 623 K and 423 K COF is significantly less than RT. The oxidation level is inadequate at 423 K at higher temperatures and is also higher than the COF tests at 623 K. The COF bends showed different sections for running and stable periods throughout 350–450 meters of sliding distance. During the run-in period, COF at RT rose to 0.7, then dropped to 0.45. During the steady state condition, there is also a fluctuation between 0.45 and 0.55. At both operating and static cycles, COF decreased, with test temperatures increasing to 423 K and 623 K. During the operating cycle, however, COF at all test temperatures is greater than static COF. The average constant state COF at RT (0.50–0.55) reduced to 0.35–0.45 and 0.25–0.35 respectively with arise in the test temperatures to 423 K and 623 K. COF, especially after 400 m, is very unstable at 623 K. In order to temporarily shield surfaces from further impact damages, Stott et al. [16] characterize the part of tribo-layers on sleeveling sides. These protective layers of glaze are continually refilled and worn down as the previous layer slides. As seen in **Figure 7**, the growth of formation, wear and reform would lead to short-term COF changes of 623 K.

3.4 Wear mechanisms for 1600 m sliding distance

The area found for sliding on the RT is smooth, with only slight abrasion, and a delamination segment (**Figure 8(a,b)**). As can be seen in **Figure 8**, highly deformed

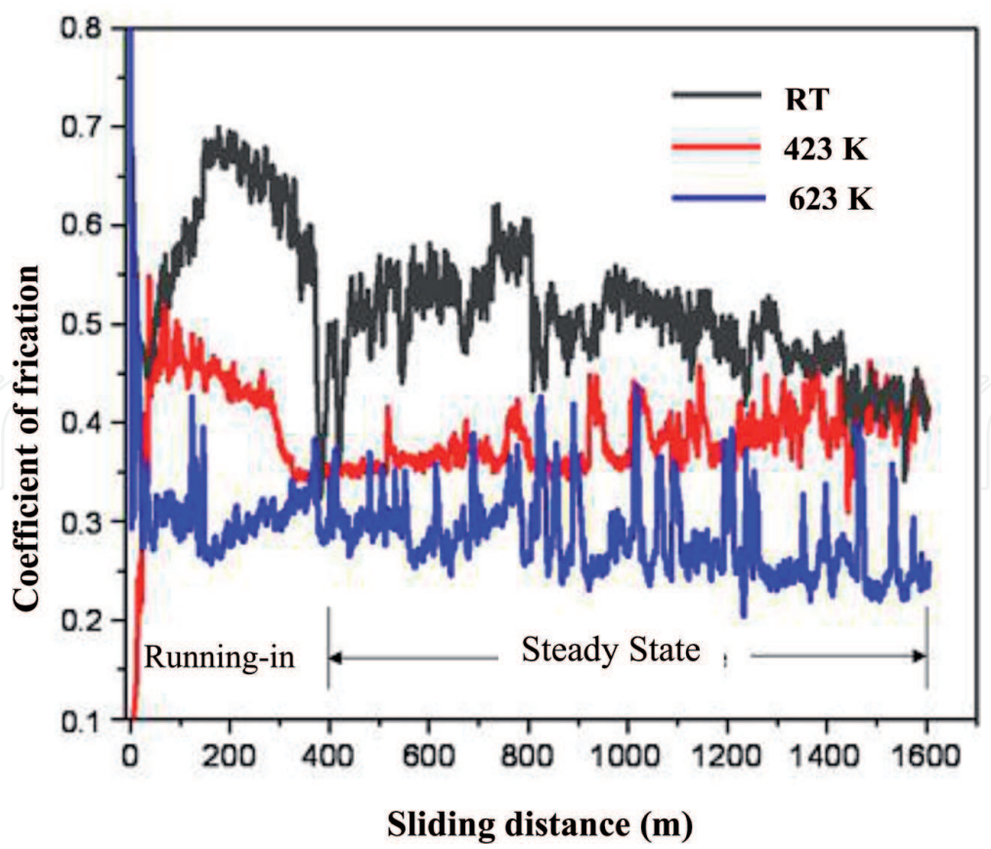

Figure 7.
Quantity of friction of the model tested at (a) RT (b) 423 K and (c) 623 K (sliding velocity 1 m/s and load 50 N).

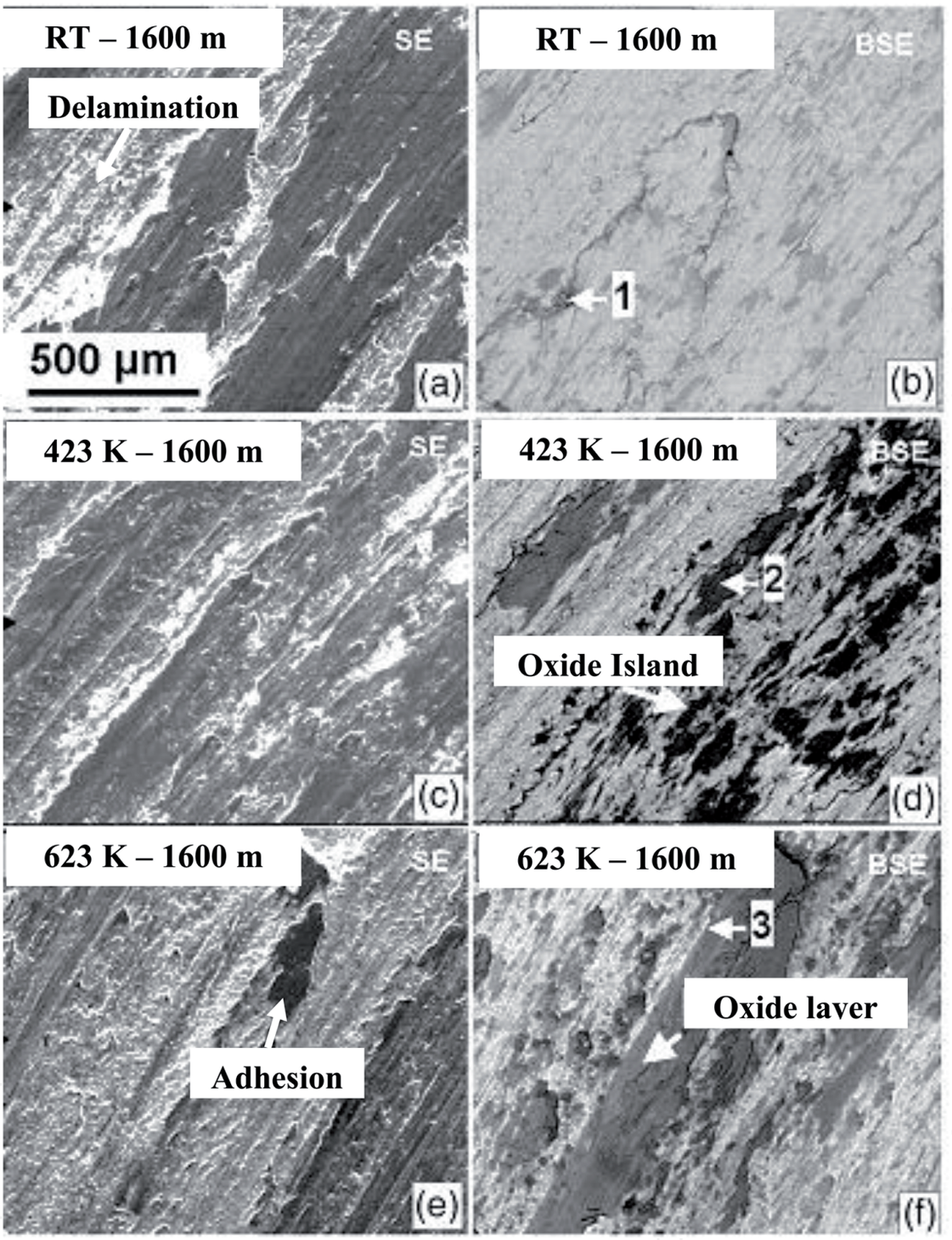

Figure 8.
SEM micrograph features of the long sliding distance worn surfaces (1600 m): (a–b) the smooth surface of the sliding RT shows delaminated portions with mild abrasive marks. (c-d) The area with mild abrasive marks of oxide islands at 423 K. (e–f) Severe 623 K coating of compacted oxide.

bits and surfaces with oxidation and minor scratches are present at this point in line with motions of the trailer (c,d). This is because the coating's spontaneous oxidation increases the output of oxide waste. The oxides on the worn area rise as the test temperature goes up to 623 K (**Figure 8(e,f)**). The wear path is oxidized more than the surface outside the contact area and therefore tribo-oxidation is required. The oxide layers are difficult enough to withstand wear and load [9].

Oxygen contained the worn surfaces, with the increase in temperature the oxygen content increased (denoted as 1, 2 and 3 in **Figure 8**). A discontinuous

oxidized film covers the worn foundation. The oxide layer composition is identical to the bulk depot composition, but at higher test temperatures, the oxygen level remains high. The distribution of the oxide layer on the tracks is not uniform. Since the processes contained in diagram as shown in **Figures 9** and **10** were interesting in 623 K, instead of RT, an attempt was made to clarify. Surfaces are divided by a slight distance in contact with each other. As sliding begins and asperities become broken and more debris development occur (**Figure 9(b)**), the shaving load reaches its limit. The processing of waste helps to minimize the interaction with asperities and quickly produces considerable waste and closes the soil.

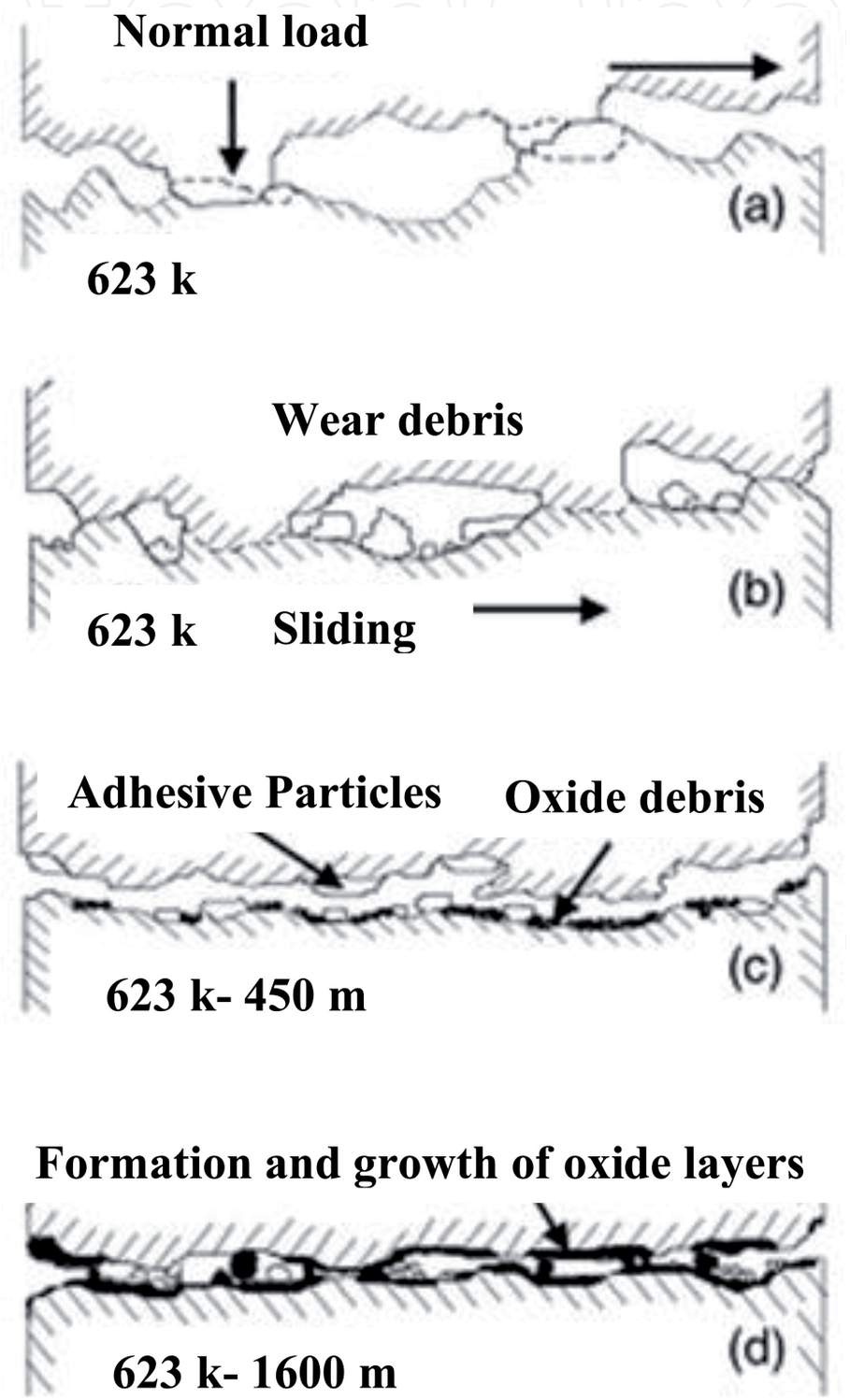

Figure 9.
Schematic representation of wear mechanisms of Colmonoy 5 deposit at RT [Ref - D. Kesavan et al. 2010].

The matrix will pluck in hard asperities, resulting in deep scratches (**Figure 9(c)**). In the other hand, debris is a third body particle that is abrasive, and causes abrasion on both directions. The slipping surfaces get smoother with time with the flat contact of the coating surface decreasing the more wear of the deposits (**Figure 9(d)**). **Figure 10(a–d)** shows the extensive wear-pathway processes at 623 K. The oxide layer prevents gradual surface wear at elevated temperatures due to its higher inherent hardening, preventing ploughing. In forming the oxide layer, the following processes are involved: Asperity fracture debris was concerned. The combination scrapping and oxidation of fine oxidized debris causes a fine tribo-layer to develop both on the

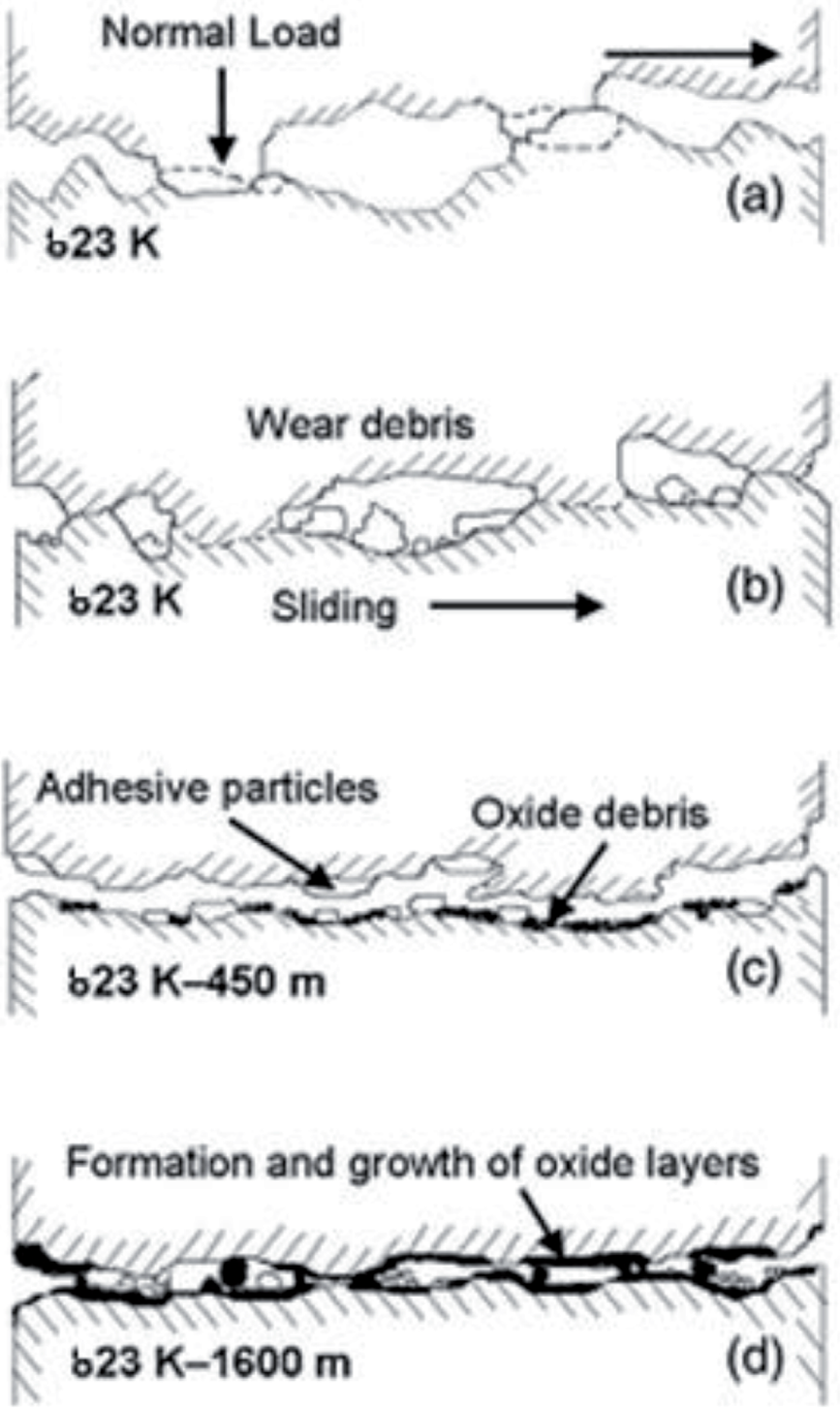

Figure 10.
Schematic representation of wear mechanisms of Colmonoy 5 deposit at 623 K [Ref - D. Kesavan eat al 2010].

surfaces of the pin and on the disc (**Figure 10(d)**). Further sliding is expected on the coating surface between tribo-layers before this tribo-layer forms. This prevents open contact between metal and metal.

4. Conclusions

1. AISI 316 L(N) austenitic stainless-steel substratum with PTA hardfaced technique was successfully deposited with nickel-based Colmonoy 5 powder at a thickness of four mm. The hardness of the deposit improved by an average of two relative to the substratum. The fact that the complicated carbides blend is spread uniformly causes the deposit to become more robust.

2. The wear loss and coefficient of friction (COF) of the deposit decrease with the rise of test temperature. The measuring temperature has a higher effect on the wear defeat of the coating than the slip space.

3. Understanding of wear loss It can be concluded that wear processes operating on the RT over the initial sliding distance is intense abrasion and tilting, according to the characteristics of the worn surface regions. In the other side, long sliding distances led to delamination and minor abrasion during wear.

4. At 423 K operating heat, mild ploughing at short sliding distances and tribo-oxidation were carried out with increasing sliding time.

5. The primary wear mechanism was adherence at the time of operating temperature at 623 K, but as the sliding distance widened, tribo-oxidation improved.

Author details

S. Gnanasekaran[1], Samson Jerold Samuel Chelladurai[2*], G. Padmanaban[3] and S. Sivananthan[4]

1 Mechanical Engineering, Sri Sakthi Institute of Engineering and Technology, Coimbatore, Tamil Nadu, India

2 Department of Mechanical Engineering, Sri Krishna College of Engineering and Technology, Coimbatore, Tamil Nadu, India

3 Centre for Materials Joining and Research (CEMAJOR), Department of Manufacturing Engineering, Annamalai University, Annamalainagar, Tamil Nadu, India

4 Mechanical Engineering, K. Ramakrishnan College of Engineering, Trichy, Tamil Nadu, India

*Address all correspondence to: samsonjeroldsamuel@skcet.ac.in

References

[1] K.L. Hsu, T.M. Ahn, D.A. Rigney, Wear 60 (1980) 13.

[2] R.L. Deuis, J.M. Yellup, C. Subramanian, Compos. Sci. Technol. 58 (1998) 299.

[3] O. Knotek, E. Lugscheider, H. Reimann, Thin Solid Films 64 (1979) 365.

[4] C.T. Kwok, F.T. Cheng, H.C. Man, Surf. Coat. Technol. 145 (2001) 206.

[5] Dawei Zhang, Xinping Zhang, Surf. Coat. Technol. 190 (2005) 212.

[6] M. Corchia, P. Delogu, F. Nenci, A. Belmondo, S. Corcoruto, W. Stabielli, Wear 119 (1987) 137.

[7] D.H.E. Persson, S. Jacobson, S. Hogmark, Wear 255 (2003) 498.

[8] A.K. Bhaduri, R. Indira, S.K. Albert, B.P.S. Rao, S.C. Jain, S. Asokkumar, J. Nucl. Mater.334 (2004) 109.

[9] H. Kashani, A. Amadeh, H.M. Ghasemi, Wear 262 (2007) 800.

[10] Seon Jin-Kim, Jun Ki-Kim, J. Nucl. Mater. 288 (2001) 163.

[11] A. Pauschitz, Manish Roy, F. Franek, Tribol. Int. 41 (2008) 584.

[12] H. Berns, Wear 181-183 (1995) 271.

[13] K. Gurumoorthy, M. Kamaraj, K. Prasad Rao, A. Sambasiva Rao, S. Venugopal, Mater. Sci. Eng. A 456(2007) 11.

[14] G.W. Stachowiak, A.W. Batchelor, Tribology Series, vol. 24, Engineering Tribology

[15] Elsevier Science Publisher, Netherlands, 1999, p. 546.

[16] F.H. Stott, Tribol. Int. 35 (2002) 489.